NASA
Technical
Paper
2025

June 1982

Static Internal Performance Characteristics of Two Thrust-Reverser Concepts for Axisymmetric Nozzles

Laurence D. Leavitt
and Richard J. Re

NASA

NASA Technical Paper 2025

1982

Static Internal Performance Characteristics of Two Thrust-Reverser Concepts for Axisymmetric Nozzles

Laurence D. Leavitt
and Richard J. Re
Langley Research Center
Hampton, Virginia

NASA
National Aeronautics
and Space Administration

Scientific and Technical Information Branch

INTRODUCTION

The design requirements for the next generation of fighter aircraft may include the ability to land on short or bomb-damaged runways. This capability will probably require adding thrust-reversing capability to nozzle designs.

The idea of thrust reversing after aircraft touchdown is certainly not new. Commercial aircraft have been using reversers during ground roll for many years. Two European tactical aircraft, the Saab-Scania Viggen and the Panavia Tornado, currently use reversers for reductions in landing ground roll. However, much of the capability of these landing-ground-roll reversers is lost by delays in deployment of the reverser upon touchdown and by the relatively long engine spool-up times required for maximum reverse thrust once aircraft touchdown has occurred. (See refs. 1 and 2.)

Additional reduction of required landing-field length might be accomplished through the use of a thrust-reversing concept which allows the pilot to maintain the engine at a high energy state by spoiling the engine thrust using a partially deployed thrust reverser. Once the aircraft has touched down, full deployment of the reverser (approximately 1 second) would provide almost instantaneous maximum reverse thrust.

Many studies on the concept of in-flight thrust reversing have been conducted in recent years. (See refs. 1 to 27.) Flight and wind-tunnel test programs on an F-94C (ref. 3), an F-100F (ref. 4), and an F-11A (refs. 5 and 7 to 11) were conducted between 1956 and 1975. These early programs demonstrated that thrust reversers integrated into single-engine axisymmetric exhaust nozzles provided many benefits, including improved flight-path control and reduced landing ground roll. However, problems were found for all cases in the handling qualities of the aircraft when the reversers were deployed at landing-approach (low-speed) conditions. Almost all the research conducted on in-flight thrust reversing for high-performance tactical aircraft since 1975 has been in conjunction with nonaxisymmetric exhaust nozzles (refs. 12 to 24, 26, and 27) with thrust-vectoring capability. If thrust vectoring is not a requirement, axisymmetric nozzles fitted with an in-flight thrust reverser may be an attractive option.

Two promising axisymmetric-nozzle thrust-reverser concepts appear to be a rotating-vane configuration (refs. 2 and 25) and a three-door configuration (ref. 2). Both concepts appear to be relatively lightweight and mechanically feasible for incorporation into a fighter aircraft. As a result, an investigation has been conducted in the static-test facility of the Langley 16-Foot Transonic Tunnel to determine the internal performance of the two thrust-reverser concepts. Nozzle exhaust was simulated using high-pressure air. Nozzle pressure ratio was varied from 2.0 to approximately 6.0.

SYMBOLS

All forces and angles are referenced to the model center line (body axis).

A_p total three-door reverser-port throat area, cm^2 (see fig. 3(b))

A_r primary nozzle-throat area on three-door reverser approach blocker, cm^2 (see fig. 3(b))

A_t total nozzle-throat area, cm^2

d_a, d_b, d_c, d_d diameters used to describe model geometry, cm (see fig. 3(b))

d_r diameter of primary nozzle throat of three-door reverser approach blocker, cm (see fig. 3(b))

F measured thrust along body axis, N

F_i ideal isentropic gross thrust, $w_p\sqrt{RT_{t,j}\left(\frac{2\gamma}{\gamma - 1}\right)\left[1 - \left(\frac{p_a}{p_{t,j}}\right)^{\frac{\gamma-1}{\gamma}}\right]}$, N

l_a, l_b, l_c, l_d, l_e lengths used to describe model geometry, cm (see fig. 3(b))

M Mach number

N measured normal force, N

p_a ambient pressure, Pa

$p_{t,j}$ average jet total pressure, Pa

R gas constant (for $\gamma = 1.3997$), 287.3 J/kg-K

$T_{t,j}$ jet total temperature, K

w width of three-door reverser port, cm (see fig. 3(b))

w_i ideal mass-flow rate, kg/sec

w_p measured mass-flow rate, kg/sec

β angle used to describe model geometry, deg (see fig. 3(b))

γ ratio of specific heats, 1.3997 for air

δ angle used to describe model geometry, deg (see fig. 3(b))

θ geometric thrust reversing angle measured from horizontal reference line, deg (see fig. 3)

λ angle used to describe model geometry, deg (see fig. 3(b))

ϕ angle used to describe model geometry, deg (see fig. 3(b))

Subscripts:

b bottom

L left

R right

t top

Abbreviations:

C-D convergent-divergent

Conf configuration

Configuration designations:

A approach

B configuration with throat-area variation

G ground roll

RV rotating vane

TD three door

APPARATUS AND METHODS

Static-Test Facility

This investigation was conducted in the static-test facility of the Langley 16-Foot Transonic Tunnel. Testing is done in a room with a high ceiling where the jet exhausts to atmosphere through a large open doorway. This facility utilizes the same clean, dry-air supply as that used in the Langley 16-Foot Transonic Tunnel and a similar air-control system, including valving, filters, and a heat exchanger (to operate the jet flow at constant stagnation temperature).

Single-Engine Propulsion Simulation System

A sketch of the single-engine air-powered nacelle model on which the thrust reversers were mounted is presented in figure 1 with a typical configuration attached.

An external high-pressure air system provided a continuous flow of clean, dry air at a controlled temperature of about 300 K. This high-pressure air was varied up to approximately 6 atm (1 atm = 101.3 kPa) and was brought through the dolly-mounted support strut by six tubes which connect to a high-pressure plenum chamber. As shown in figure 1, the air was then discharged perpendicularly into the model low-pressure plenum through eight multiholed sonic nozzles equally spaced around the high-pressure plenum. This method was designed to minimize any forces imposed by the transfer of axial momentum as the air is passed from the nonmetric (not mounted to the force

balance) high-pressure plenum to the metric (mounted to the force balance) low-pressure plenum. Two flexible metal bellows are used as seals and serve to compensate for axial forces caused by pressurization.

The air was then passed from the model low-pressure plenum through a transition section, choke plate, and instrumentation section, which were common for all reverser configurations investigated. All reverser configurations were attached to the instrumentation section at model station 97.49 cm.

Nozzle Design

Photographs of the two axisymmetric-nozzle thrust-reverser concepts are shown in figure 2, and sketches are presented in figure 3. A summary of configurations tested is shown below:

Conf	Type	Operating mode	θ, deg	θ_t, deg	θ_b, deg	Port area
RV1	Rotating vane	Approach		50	50	Baseline
RV1B	↓	↓		50	50	Reduced
RV2	↓	↓		70	70	Baseline
RV3	↓	↓		90	90	↓
RV4	↓	Ground roll		110	110	↓
RV5	↓	↓		130	130	↓
RV5B	↓	↓		130	130	Reduced
RV6	↓	Approach		50	90	Baseline
TD120A	Three door	↓	120			↓
TD130A	↓	↓	130			↓
TD130AB	↓	↓	130			Reduced
TD140A	↓	↓	140			Baseline
TD120G	↓	Ground roll	120			↓
TD130G	↓	↓	130			↓
TD130GB	↓	↓	130			Reduced
TD140G	↓	↓	140			Baseline

The rotating-vane concept (figs. 2(a) and 3(a)) represents a thrust-reverser concept in which reversing is accomplished upstream of the nozzle throat. When the reverser is deployed, a set of internal clamshell blockers (represented by the blocker plate in fig. 3(a)) is completely closed. This directs all the exhaust flow out through the vanes, while allowing the engine to remain "spooled up" in case of a missed approach. The vanes are rotated aft or forward depending on the level of thrust reversing or spoiling required. In the approach mode, the vanes are rotated aft ($\theta < 90°$) to direct the exhaust flow away from empennage control surfaces, thus maintaining empennage control effectiveness while spoiling thrust. Once the aircraft has touched down, the vanes can be rotated forward (to $\theta = 130°$) for maximum deceleration capability.

The hardware of the rotating-vane model tested does not represent the external geometry of a rotating-vane thrust reverser integrated into an axisymmetric nozzle. However, since all tests were conducted at static conditions, it is not required to simulate external geometry. Internal geometry, on the other hand, was accurately simulated upstream of the blocker plate. (See fig. 3(a).) The blocker-plate geome-

try was somewhat different than the internal clamshell blocker of the actual rotating-vane reverser design concept; however, it is believed that the effects of this variation are relatively small. Note also in figure 3(a) that two of the rotating-vane configurations, RV1B and RV5B (or "B" configurations), were simply variations in throat area A_t of configurations RV1 and RV5, respectively. These area changes were accomplished by placing shims (not shown) along the sides of the reverser port openings, which reduced the port width from 8.31 cm to approximately 7.65 cm.

The three-door reverser concept (figs. 2(b) and 3(b)), unlike the rotating-vane concept, provides reversing downstream of the unreversed nozzle throat. This concept may be advantageous because it places the reversing port farther away from the empennage control surfaces. Both approach and ground-roll geometries were tested, as was the case with the rotating-vane reverser. For approach configurations, part of the exhaust flow is directed forward through the three reverser ports, and the rest is directed aft through the primary nozzle. The amount of thrust spoiling, or reversing, can be regulated by varying the internal clamshell position. Geometries of the approach blockers and ground-roll blockers are included in figure 3(b).

Reverser-port area variations on the three-door 130° approach (TD130A) and 130° ground-roll (TD130G) configurations were tested (TD130AB and TD130GB, respectively). Reverser-port area reduction was accomplished by placing shims (not shown) upstream of the throat inserts (fig. 3(b)) in each port. These shims moved the throat insert downstream, resulting in a reduction in w. Also, figure 3(b) shows that A_r refers to the throat area of the primary nozzle on the approach configurations.

Instrumentation

Forces and moments on the model downstream of station 52.07 cm were measured by a three-component strain-gage balance. Jet total pressure was measured at a fixed station in the instrumentation section by means of a five-probe rake (see fig. 1) and a single probe (not shown). Each probe was weighted using constants determined by surveying the nozzle-exit flow of two standard-calibration nozzles tested prior to testing the reverser configurations. A thermocouple, also located in the instrumentation section, was used to measure jet total temperature. Total mass-flow properties were determined based on temperature and pressure measurements made in the supply pipe upstream of the eight sonic nozzles. These measurements were used to calibrate the discharge coefficients of the sonic nozzles against known discharge coefficients of standard convergent choke nozzles as discussed in reference 16.

Several pressure tubes were secured externally to the model and propulsion system to determine whether a correction would be required for effects of the jet on any external surfaces. Negligible effects of the jet on external pressures were found, hence no correction was applied to the data.

Data Reduction

All data were recorded on magnetic tape. At each test point, approximately 50 frames of data were recorded at a rate of 10 frames per second. These samples were averaged, and the averaged values were used for all computations. All data included in this report are referenced to the model center line.

The basic performance parameter used for the presentation of results is the internal thrust ratio F/F_i, which is the ratio of the actual nozzle thrust (along the body axis) to the ideal nozzle thrust. Actual nozzle thrust was obtained from the balance axial-force measurement corrected for weight tares and balance interactions. Although the bellows arrangement was designed to eliminate pressure and momentum interactions with the balance, small bellows tares on axial, normal, and pitch balance components still exist. These tares result from a small pressure difference between the ends of the bellows when internal velocities are high and also from small differences in the forward- and aft-bellows spring constants when the bellows are pressurized. As discussed in reference 16, these bellows tares were determined by running convergent calibration nozzles with known performance over a range of expected normal forces and pitching moments. The balance data were then corrected in a manner similar to that discussed in reference 16.

RESULTS AND DISCUSSION

The variation of nozzle discharge coefficient w_p/w_i and internal thrust ratio F/F_i with nozzle pressure ratio (ratio of jet total pressure to ambient pressure) for each reverser configuration is presented in figures 4 and 5. Figures 4(b) and 5(b) present variations of the ratio of measured normal force to ideal thrust with nozzle pressure ratio for each configuration tested.

The ideal mass-flow rate w_i (used in the discharge-coefficient calculation) was for all configurations based on the actual measured reverser throat (or port) areas. These throat areas vary for each configuration tested. (See fig. 3.)

Rotating-Vane Reverser

A summary of measured discharge coefficients w_p/w_i for the rotating-vane reverser is shown in figure 4(a). These discharge coefficients are low in magnitude compared with typical forward-mode nozzle operation and are not independent of nozzle pressure ratio. Both of these observations seem to indicate the possibility of flow-separation regions in the reverser ports. These regions could result in sonic flow areas which are substantially less than measured geometric throat areas and which vary with nozzle pressure ratio and reverser-vane angle. Discharge coefficient generally decreased as reverser angle decreased from 130° (reversed thrust) to 50° (spoiled thrust). This result is believed to be caused by orientation of the reverser vanes relative to the reverser port. As shown in figure 3(a), the reverser-port forward and aft walls are aligned at 130° from the horizontal reference line and are therefore aligned with the vanes for configuration RV5 (θ_t/θ_b = 130°/130°). As the rotating vanes are rotated aft toward θ = 50°, the reverser flow is redirected from a flow angle of approximately 130° in the reverser port back toward the thrust axis. This results in additional discharge-coefficient losses.

The two iterations on reverser-port area (reduced port area), configurations RV1B (θ = 50°) and RV5B (θ = 130°), resulted in an increase in discharge coefficient. The reason for this increase is not fully understood, but it may be the result of the area-reduction shims being placed in regions of flow separation (low energy flow). This results in a reduction of the internal flow losses. These area-reduction shims may also result in a more well-defined or stable choke (sonic) line for the throat. Another interesting (and at the present, unexplainable) observation results from comparing discharge coefficients of the asymmetric reverser configuration RV6 (θ_t/θ_b = 50°/90°) with those of configurations RV1 (θ = 50°) and RV3 (θ = 90°). For

all nozzle pressure ratios tested, the discharge coefficients of reverser configuration RV6 were higher than those of configurations RV1 or RV3. This was surprising in that reverser RV6 discharge coefficients would be expected to fall between those of RV1 and RV3. It can only be assumed that asymmetric reversing must significantly alter the internal flow patterns and throat (choke) location and area.

A summary of the internal thrust-ratio performance characteristics for the rotating-vane reverser is also shown in figure 4(a). For purposes of comparison, the ideal value of F/F_i based on the cosine of the reverser angle (cos θ) is also presented. As can be seen, varying amounts of thrust spoiling or reverse thrust are provided, depending upon turning-vane angle. In general, for all vane configurations tested, F/F_i increased as nozzle pressure ratio $p_{t,j}/p_a$ increased, indicating a reduction in reversing effectiveness with increasing nozzle pressure ratio. The 50° approach configuration RV1 spoils thrust more effectively than would be expected by the vane angle (cos 50° = 0.64). This is due to the inability of the turning vanes to efficiently redirect the reverser-port exhaust flow (which is aligned at approximately 130°) aft. The 130° ground-roll configuration RV5 provided the largest amount of reverse thrust, as expected, and exceeded the "desired" level of $F/F_i = -0.5$ (ref. 12) for all nozzle pressure ratios tested.

The effect of reduced port area (throat area) on static internal thrust performance is also shown in figure 4(a). As expected, small reductions in reverser-port area had little effect on internal thrust-ratio performance.

Asymmetric reversing configuration RV6 (θ_t/θ_b = 50°/90°) resulted in a spoiled thrust-ratio performance level between that of configurations RV1 (θ_t/θ_b = 50°/50°) and RV3 (θ_t/θ_b = 90°/90°). However, the internal thrust-ratio performance of configuration RV6 indicates that more thrust was spoiled than would have been calculated ($F/F_i = 0.32$) based on reverser geometry. Again, this is due to the decreased turning efficiency of the $\theta = 50°$ vanes, allowing more exhaust flow to be passed through the $\theta = 90°$ vanes than through the $\theta = 50°$ vanes.

The ratios of measured normal force to ideal thrust (fig. 4(b)) for configuration RV6 also indicate that more exhaust flow was passed through the $\theta = 90°$ vanes than through the $\theta = 50°$ vanes. Had equal amounts of mass flow been exhausted from the 50° top-port and 90° bottom-port turning vanes, a value of N/F_i of approximately 0.12 would have resulted (based on summation of force components). As shown in figure 4(b), values of N/F_i in excess of 0.24 were obtained. These values of N/F_i are in general greater than the internal thrust ratios F/F_i, and large nose-down pitching moments can be generated when the reverser is not located at the aircraft pitch center.

Three-Door Reverser

A summary of the measured discharge coefficients for the three-door reverser is presented in figure 5(a). As was the case with the rotating-vane reverser, discharge coefficients are generally low and are not independent of nozzle pressure ratio. The three-door reverser discharge coefficients fall into two distinct groups. As expected, the approach-configuration data are significantly higher in magnitude than the ground-roll configurations, because less than 50 percent of the exhaust flow is directed out the reverser ports. The remainder is exhausted axially through the primary nozzle. The approach-configuration discharge coefficients agreed to within approximately 1 percent, at a constant value of $p_{t,j}/p_a$, except for the area iteration on the 130° approach reverser case. Discharge coefficient was between 1

and 2 percent higher for configuration TD130AB (smaller port area), because a larger percentage of the total exhaust flow was directed through the more efficient primary nozzle. The reduced area of the ground-roll reverser configuration TD130GB also provided increases in discharge coefficient when compared with configuration TD130G. Reasons for the increase are unknown, but could result from improved internal flow conditions (possibly reduced internal separation). Static internal thrust performance for the three-door reverser configurations is also presented in figure 5(a). Forward thrust was spoiled for all approach configurations tested. Thrust ratio F/F_i for the approach configurations are nearly linear and increase (reduced reverser efficiency) only slightly with increasing nozzle pressure ratio. The 140° approach configuration TD140A was the only exception. No loss in reverse-thrust performance with increasing values of $p_{t,j}/p_a$ was experienced. A reduction in reverser-port area for the 130° approach reverser configuration TD130AB resulted in a 2 to 3 percent loss in reverse thrust. This is the result of a larger portion of the exhaust flow exiting through the primary nozzle as compared with the configuration TD130A.

The ground-roll reverser configurations all provided amounts of reverse thrust in excess of $F/F_i = -0.5$, except for the 120° configuration TD120G for values of $p_{t,j}/p_a < 3.0$. As shown in figure 5(a), reverse-thrust performance of the ground-roll configuration was dependent upon jet total-pressure ratio $p_{t,j}/p_a$. Peak reverse-thrust performance occurred between a nozzle pressure ratio of 3.5 and 4.0. These peaks are believed to be the result of supersonic expansion downstream of the throat in the reverser duct. This expansion may be the result of one or more of the following factors: (1) A small amount of divergence downstream of the reverser-port throats caused by the radial shape of the port openings, (2) external expansion on the throat insert downstream of the reverser-port throats, or (3) internal flow separation around the reverser duct corners.

Only one data point could be obtained on configuration TD140G (140° ground-roll reverser) because of severe model vibrations encountered when nozzle pressure ratio was increased from $p_{t,j}/p_a = 2.0$. These severe vibrations are believed to be related to unsteady separation regions at the entrance corners of the reverser passages. The oscillations in the nozzle were so severe that they fed forward into the cylindrical instrumentation section and were observed on the jet total-pressure rake readings. These vibrations would have to be eliminated for practical application for aircraft use. However, since TD130G ($\theta = 130°$) provided levels of reverse thrust in excess of -0.5, there seems to be little need for configuration TD140G.

The ratio of measured normal force to ideal thrust versus nozzle pressure ratio for the three-door reverser configurations is presented in figure 5(b). It is shown in the figure that there are some relatively large normal-force components (especially for configurations TD130G and TD130GB). For these configurations, undesirable normal-force components could probably be eliminated by simply adjusting port areas (for example, reducing the top-port throat area).

Performance Comparisons

A comparison of the measured thrust ratios F/F_i with the maximum expected thrust ratio based on geometric reverser angle θ is presented in figure 6. The maximum expected thrust ratio (represented by the solid line) is simply defined as the cosine of the geometric reverser angle. Perhaps the most correct way to define the maximum expected thrust ratio for thrust-reverser configurations (vane angles, etc.) of a particular generic nozzle type would be to multiply $\cos\theta$ by F/F_i for

the unreversed baseline nozzle. This would result in maximum expected thrust ratios that are biased toward the actual thrust ratio of the baseline nozzle. For this study, the value of unreversed baseline nozzle F/F_i was assumed to be 1.0, since several different nozzle types from several references are compared. With the variable-geometry, high-performance nozzles currently existing (or being studied), this assumption is a reasonable one and has little effect on the results presented. Values of thrust ratio above the expected thrust-ratio curve (solid line in fig. 6) represent reduced reversing efficiency (or an actual reverse-thrust turning angle smaller than the geometric reversing angle). Conversely, values of thrust ratio below the expected thrust-ratio curve indicate more reverse thrust than expected. Comparisons are made at a nozzle pressure ratio of 2.6, which is typical of current high-performance, low-bypass-ratio engines operating at approach and landing conditions. As shown in figure 6, comparisons are made between the rotating-vane and three-door reversers of the present investigation and several other thrust-reverser concepts including axisymmetric, two-dimensional convergent-divergent (2-D C-D), and wedge nozzle reverser concepts.

The thrust ratios for the rotating-vane and three-door reversers are, in general, close to the expected values, indicating relatively efficient thrust-reversing operations compared with many of the other thrust-reversing concepts. In fact, the rotating-vane reverser provided more reverse thrust than expected for $\theta \leq 110°$. A curve faired through the data for the rotating-vane reverser intersects the calculated thrust-ratio curve at approximately $\theta = 115°$. This indicates that the reverser exhaust probably tends to exit the reverser port at an angle of 115°, rather than aligning itself with the reverser-port walls at $\theta = 130°$. This argument explains why the thrust ratios for rotating-vane angles less than 110° provide more reverse thrust than expected and why vane angles greater than 110° provide less reverse thrust than expected. Both the rotating-vane and three-door reverser concepts were capable of providing reverse-thrust ratios in excess of the desired $F/F_i = -0.5$ for maximum ground-roll deceleration effectiveness.

SUMMARY OF RESULTS

An investigation has been conducted in the static-test facility of the Langley 16-Foot Transonic Tunnel to determine the static performance of two axisymmetric-nozzle thrust-reverser concepts. A rotating-vane thrust reverser represented a concept in which reversing is accomplished upstream of the nozzle throat, and a three-door reverser concept provided reversing downstream of the nozzle throat. Nozzle pressure ratio was varied from 2.0 to approximately 6.0. The results of this investigation indicate the following:

1. Both the rotating-vane and three-door reverser concepts were capable of providing static reverse-thrust ratios in excess of -0.5 for maximum landing-ground-roll deceleration effectiveness.

2. Both the rotating-vane and three-door reverser concepts were effective static thrust spoilers with the landing-approach (forward-flight) nozzle geometry.

3. Comparisons of measured static thrust ratios with expected thrust ratios based on geometric turning angle indicate relatively efficient reverser performance for both reverser concepts. Magnitudes of reverse-thrust ratio for a given geometric reverser angle for the two axisymmetric reversers of this study were generally equal to or greater than the magnitudes of reverse-thrust ratio measured on other types of thrust reversers.

Langley Research Center
National Aeronautics and Space Administration
Hampton, VA 23665
April 30, 1982

REFERENCES

1. Lorincz, Dale J.; Chiarelli, Charles; and Hunt, Brian L.: Effect of In-Flight Thrust Reverser Deployment on Tactical Aircraft Stability and Control. AIAA 81-1446, July 1981.

2. Blackman, J. P.; and Eigenmann, M. F.: Axisymmetric Approach and Landing Thrust Reversers. AIAA 81-1650, Aug. 1981.

3. Anderson, Seth B.; Cooper, George E.; and Faye, Alan E., Jr.: Flight Measurements of the Effect of a Controllable Thrust Reverser on the Flight Characteristics of a Single-Engine Jet Airplane. NASA MEMO 4-26-59A, 1959.

4. Kelly, Mark W.; Greif, Richard K.; and Tolhurst, William H., Jr.: Full-Scale Wind-Tunnel Tests of a Swept-Wing Airplane With a Cascade-Type Thrust Reverser. NASA TN D-311, 1960.

5. Simpson, W. R.; Covey, M. W.; Palmer, D. F.; and Hewett, M. D.: Navy Evaluation of F-11A In-Flight Thrust Control System. SA-75R-75, U.S. Naval Air Test Center, Dec. 15, 1975. (Available from DTIC as AD A019 954.)

6. Steffen, Fred W.; and McArdle, Jack G.: Performance Characteristics of Cylindrical Target-Type Thrust Reversers. NACA RM E55I29, 1956.

7. Swihart, John M.: Effect of Target-Type Thrust Reverser on Transonic Aerodynamic Characteristics of a Single-Engine Fighter Model. NACA RM L57J16, 1958.

8. Weiss, D. C.; and McGuigan, W. M.: Inflight Thrust Control for Fighter Aircraft. AIAA Paper No. 70-513, Mar. 1970.

9. Linderman, D. L.; and Mount, J. S.: Development of an In-Flight Thrust Reverser for Tactical/Attack Aircraft. AIAA Paper No. 70-699, June 1970.

10. Maiden, Donald L.; and Mercer, Charles E.: Performance Characteristics of a Single-Engine Fighter Model Fitted With an In-Flight Thrust Reverser. NASA TN D-6460, 1971.

11. Mercer, Charles E.; and Maiden, Donald L.: Effects of an In-Flight Thrust Reverser on the Stability and Control Characteristics of a Single-Engine Fighter Airplane Model. NASA TN D-6886, 1972.

12. Hiley, P. E.; Wallace, H. W.; and Booz, D. E.: Nonaxisymmetric Nozzles Installed in Advanced Fighter Aircraft. J. Aircr., vol. 13, no. 12, Dec. 1976, pp. 1000-1006.

13. Goetz, Gerald F.; Young, John H.; and Palcza, J. Lawrence: A Two-Dimensional Airframe Integrated Nozzle Design With Inflight Thrust Vectoring and Reversing Capabilities for Advanced Fighter Aircraft. AIAA Paper No. 76-626, July 1976.

14. Capone, Francis J.; and Maiden, Donald L.: Performance of Twin Two-Dimensional Wedge Nozzles Including Thrust Vectoring and Reversing Effects at Speeds up to Mach 2.20. NASA TN D-8449, 1977.

15. Willard, C. M.; Capone, F. J.; Konarski, M.; and Stevens, H. L.: Static Performance of Vectoring/Reversing Non-Axisymmetric Nozzles. AIAA Paper 77-840, July 1977.

16. Capone, Francis J.: Static Performance of Five Twin-Engine Nonaxisymmetric Nozzles With Vectoring and Reversing Capability. NASA TP-1224, 1978.

17. Hiley, P. E.; Kitzmiller, D. E.; and Willard, C. M.: Installed Performance of Vectoring/Reversing Nonaxisymmetric Nozzles. J. Aircr., vol. 16, no. 8, Aug. 1979, pp. 532-538.

18. Capone, Francis J.; Gowadia, Nashir S.; and Wooten, W. H.: Performance Characteristics of Nonaxisymmetric Nozzles Installed on the F-18 Aircraft. AIAA Paper 79-0101, Jan. 1979.

19. Petit, John E.; and Capone, Francis J.: Performance Characteristics of a Wedge Nozzle Installed on an F-18 Propulsion Wind Tunnel Model. AIAA Paper 79-1164, June 1979.

20. Capone, Francis J.: The Nonaxisymmetric Nozzle - It is For Real. AIAA Paper 79-1810, Aug. 1979.

21. Laughrey, J. A.; Drape, D. J.; and Hiley, P. E.: Performance Evaluation of an Air Vehicle Utilizing Nonaxisymmetric Nozzles. AIAA Paper 79-1811, Aug. 1979.

22. Capone, Francis J.; and Berrier, Bobby L.: Investigation of Axisymmetric and Nonaxisymmetric Nozzles Installed on a 0.10-Scale F-18 Prototype Airplane Model. NASA TP-1638, 1980.

23. Bare, E. Ann; Berrier, Bobby L.; and Capone, Francis J.: Effects of Simulated In-flight Thrust Reversing on Vertical-Tail Loads of F-18 and F-15 Airplane Models. NASA TP-1890, 1981.

24. Capone, Francis J.; Re, Richard J.; and Bare, E. Ann: Thrust Reversing Effects on Twin-Engine Aircraft Having Nonaxisymmetric Nozzles. AIAA-81-2639, Dec. 1981.

25. Banks, D. W.; Quinto, P. F.; and Paulson, J. W., Jr.: Thrust-Induced Effects on Low-Speed Aerodynamics of Fighter Aircraft. AIAA-81-2612, Dec. 1981.

26. Re, Richard J.; and Berrier, Bobby L.: Static Internal Performance of Single Expansion-Ramp Nozzles With Thrust Vectoring and Reversing. NASA TP-1962, 1982.

27. Hiley, P. E.; and Bowers, D. L.: Advanced Nozzle Integration for Supersonic Strike Fighter Application. AIAA-81-1441, July 1981.

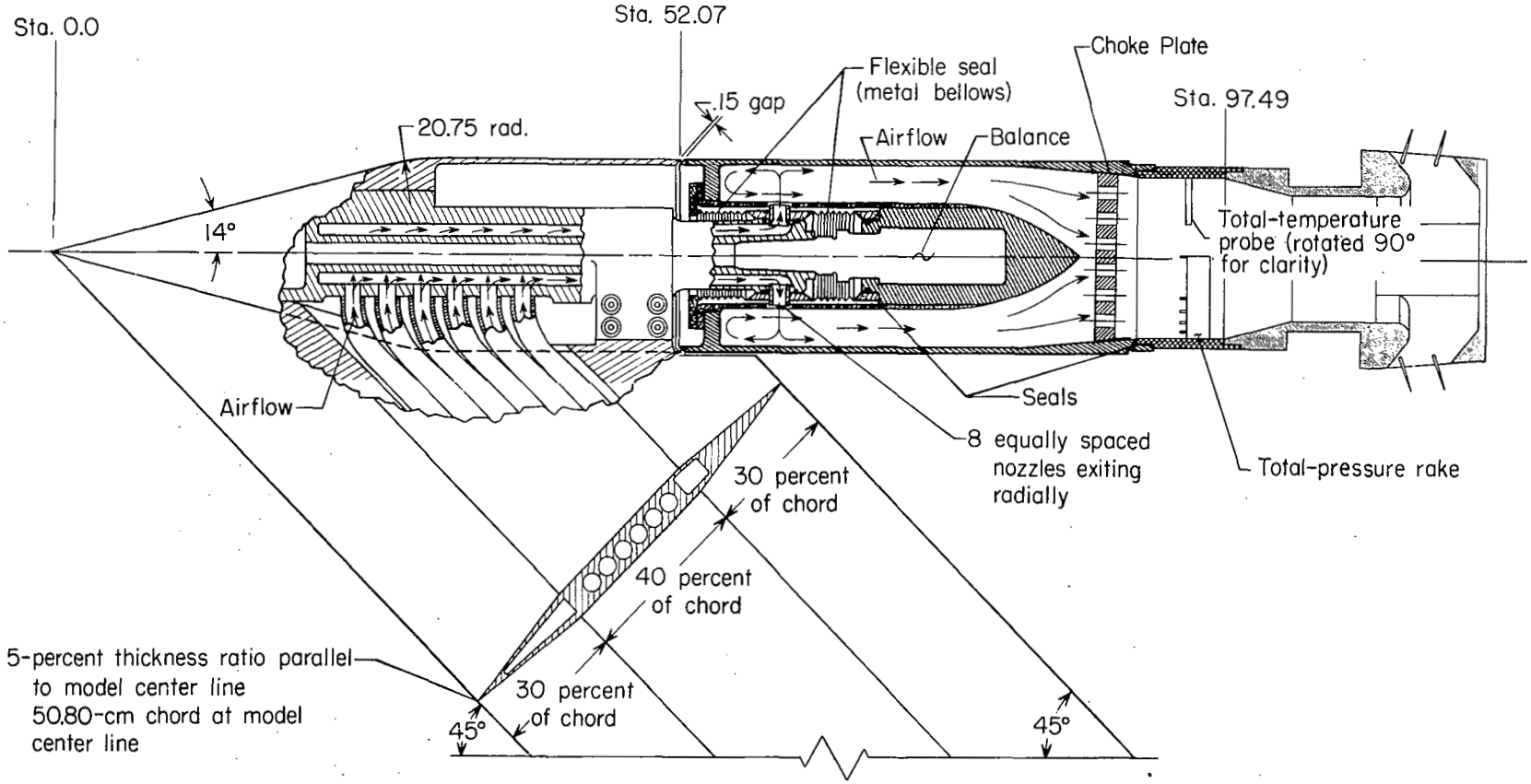

Figure 1.- Sketch showing general arrangement of air-powered single-engine nacelle model. (All dimensions in cm unless otherwise noted.)

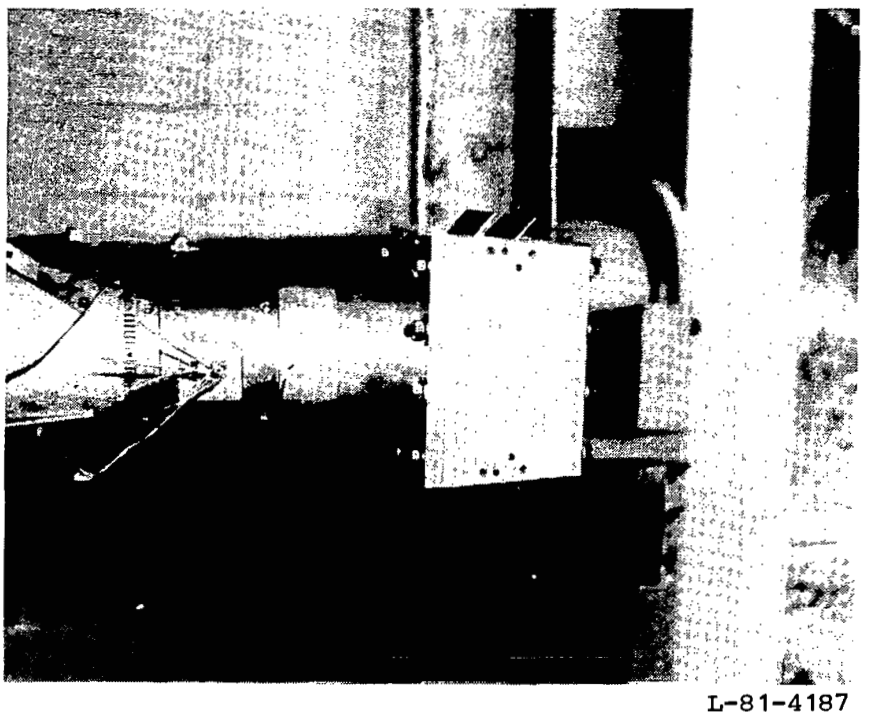

L-81-4187

(a) Rotating-vane thrust reverser; θ_t/θ_b = 50°/50°; configuration RV1.

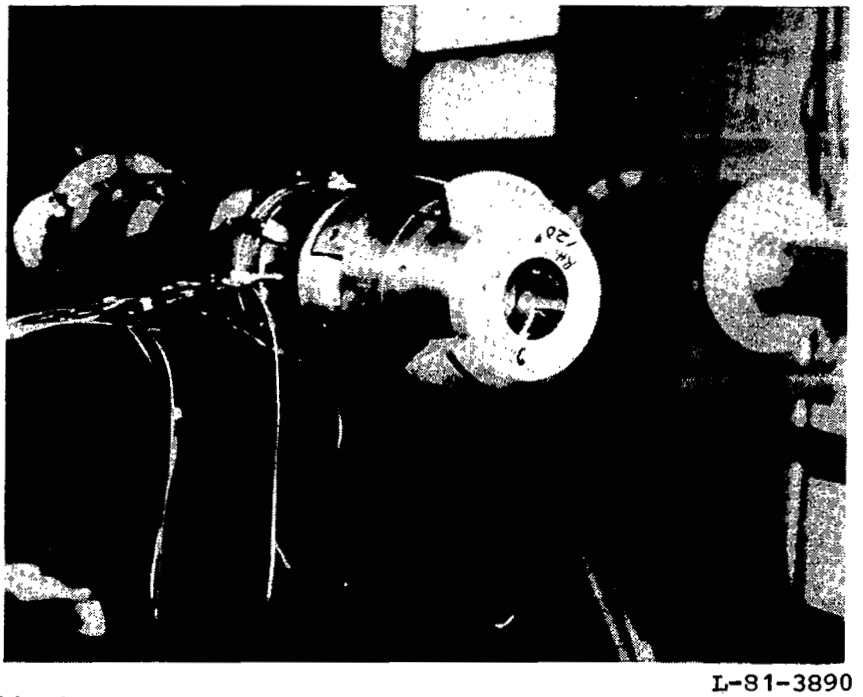

L-81-3890

(b) Three-door thrust reverser; 120° approach geometry; configuration TD120A.

Figure 2.- Photographs of axisymmetric-nozzle thrust reversers installed in static-test facility of Langley 16-Foot Transonic Tunnel.

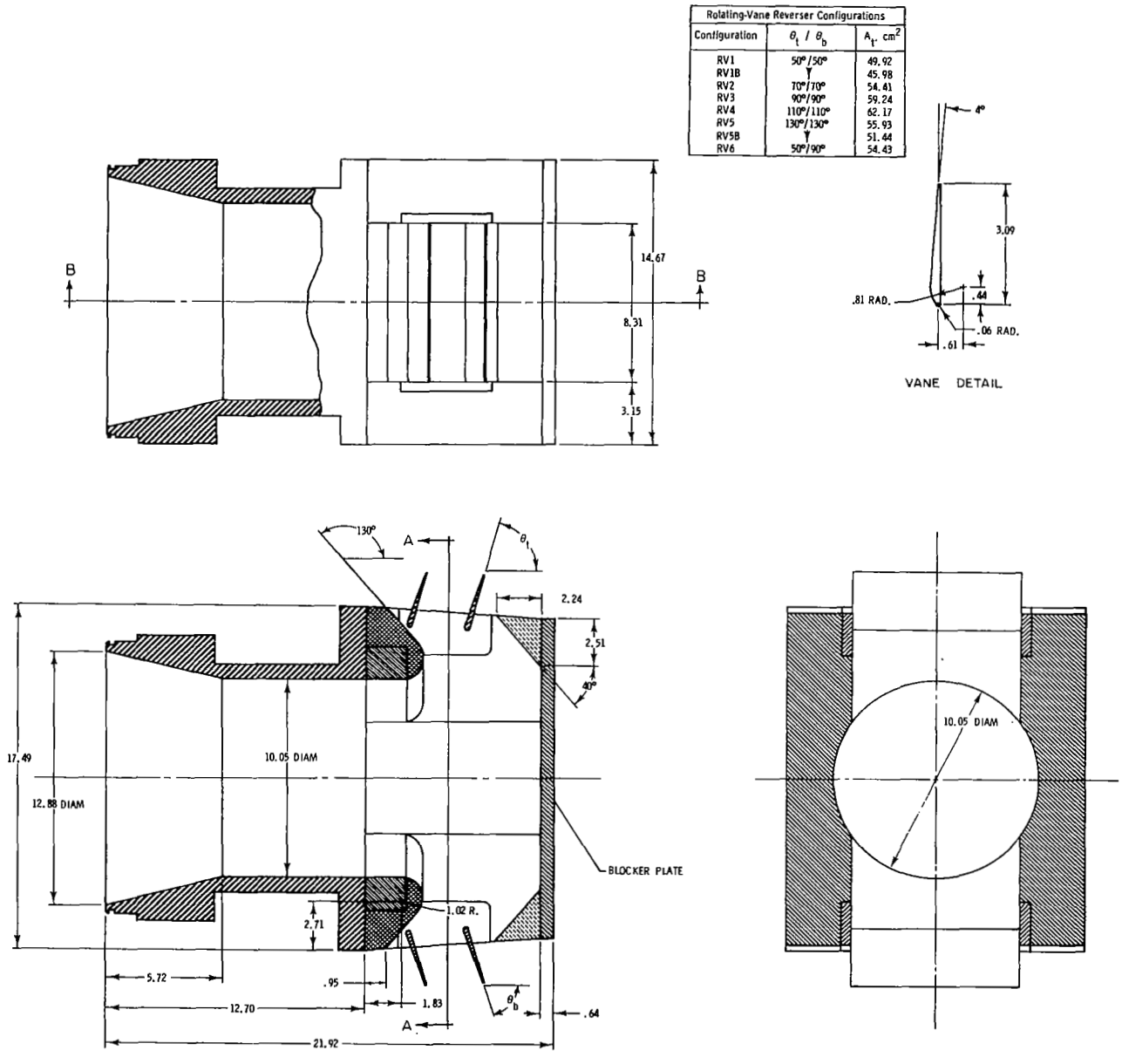

(a) Rotating-vane thrust reverser.

Figure 3.- Sketches of axisymmetric thrust-reverser concepts. (All dimensions in cm unless otherwise noted.)

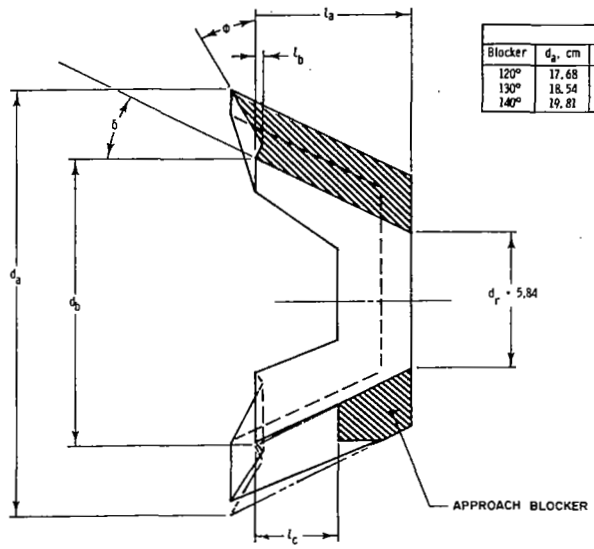

Approach Blocker Geometry							
Blocker	d_a, cm	d_b, cm	l_a, cm	l_b, cm	l_c, cm	δ, deg	Φ, deg
120°	17.68	12.60	4.91	.30	3.46	34.5	25.5
130°	18.54	12.50	6.67	.30	3.53	26.5	30.0
140°	19.81	12.24	7.73	.30	3.31	22.5	22.5

Three-Door Reverser Configurations							
Configuration	θ, deg	w_t, cm	w_R, cm	w_L, cm	A_p, cm^2	A_r, cm^2	A_t, cm^2
TD120A	120	1.35	1.34	1.33	25.21	26.81	52.02
TD130A	130	1.33	1.32	1.32	24.89	↓	51.70
TD130AB	↓	1.23	1.23	1.22	23.07	↓	49.88
TD140A	140	1.34	1.33	1.33	25.16	↓	51.97
TD120G	120	2.99	2.99	2.98	56.19	0.0	56.19
TD130G	130	2.97	2.99	2.97	55.97	↓	55.97
TD130GB	↓	2.92	2.90	2.93	54.86	↓	54.86
TD140G	140	2.97	2.98	2.98	55.92	↓	55.92

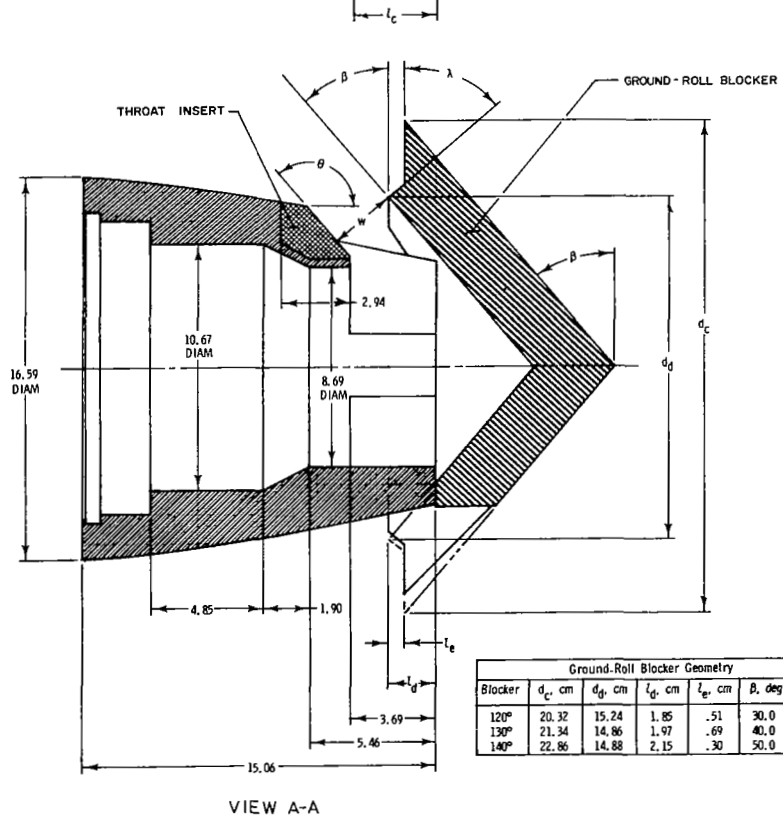

VIEW A-A

Ground-Roll Blocker Geometry						
Blocker	d_c, cm	d_d, cm	l_d, cm	l_e, cm	β, deg	λ, deg
120°	20.32	15.24	1.85	.51	30.0	60.0
130°	21.34	14.86	1.97	.69	40.0	50.0
140°	22.86	14.88	2.15	.30	50.0	40.0

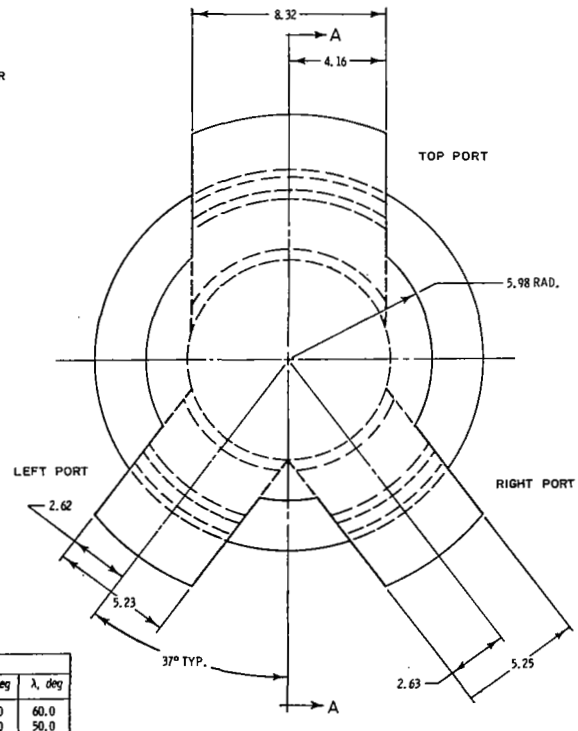

(b) Three-door thrust reverser.

Figure 3.- Concluded.

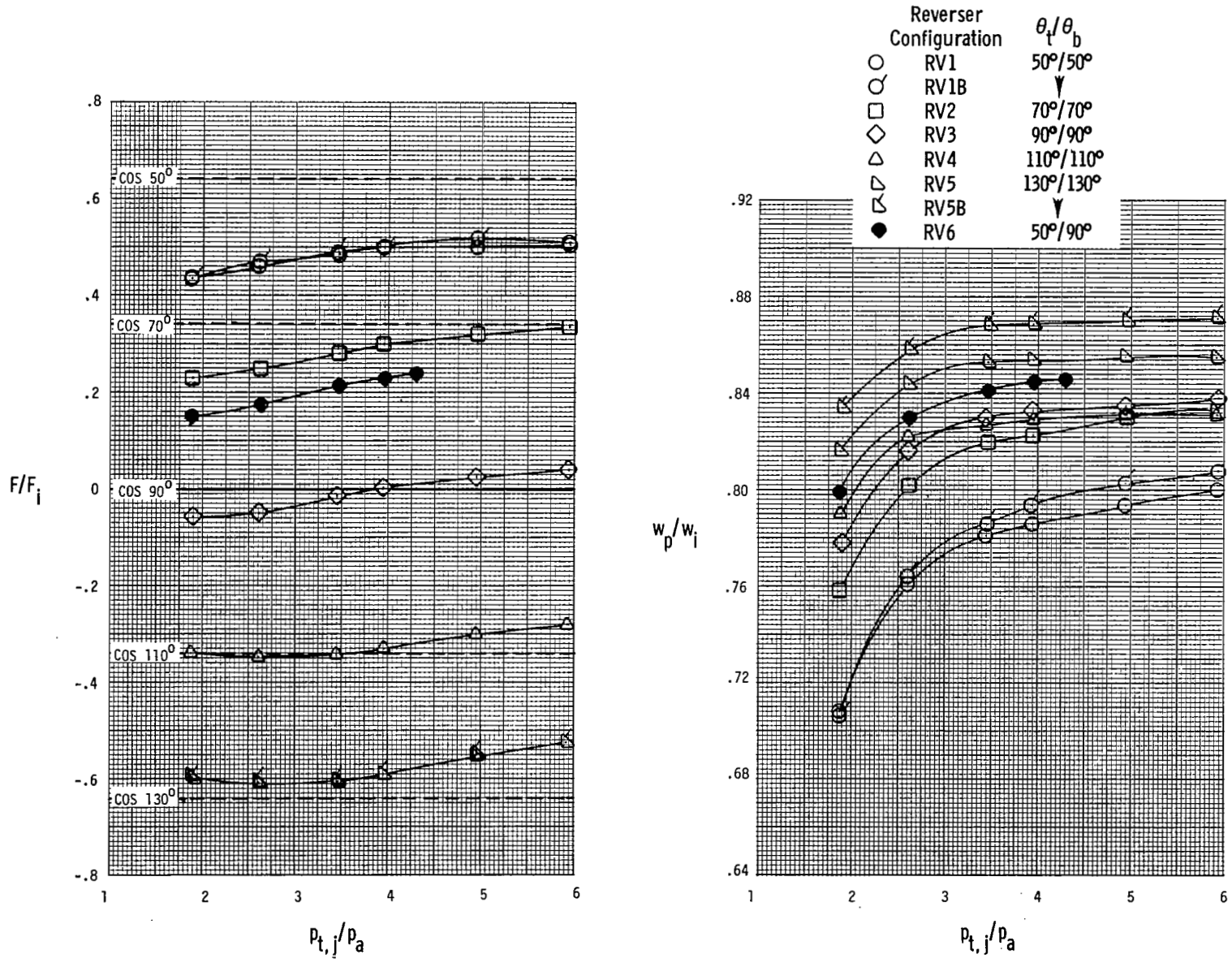

(a) Thrust ratio and discharge coefficient.

Figure 4.- Summary of static (M = 0) performance characteristics of rotating-vane thrust-reverser concept. Tick marks represent area iterations ("B" configurations).

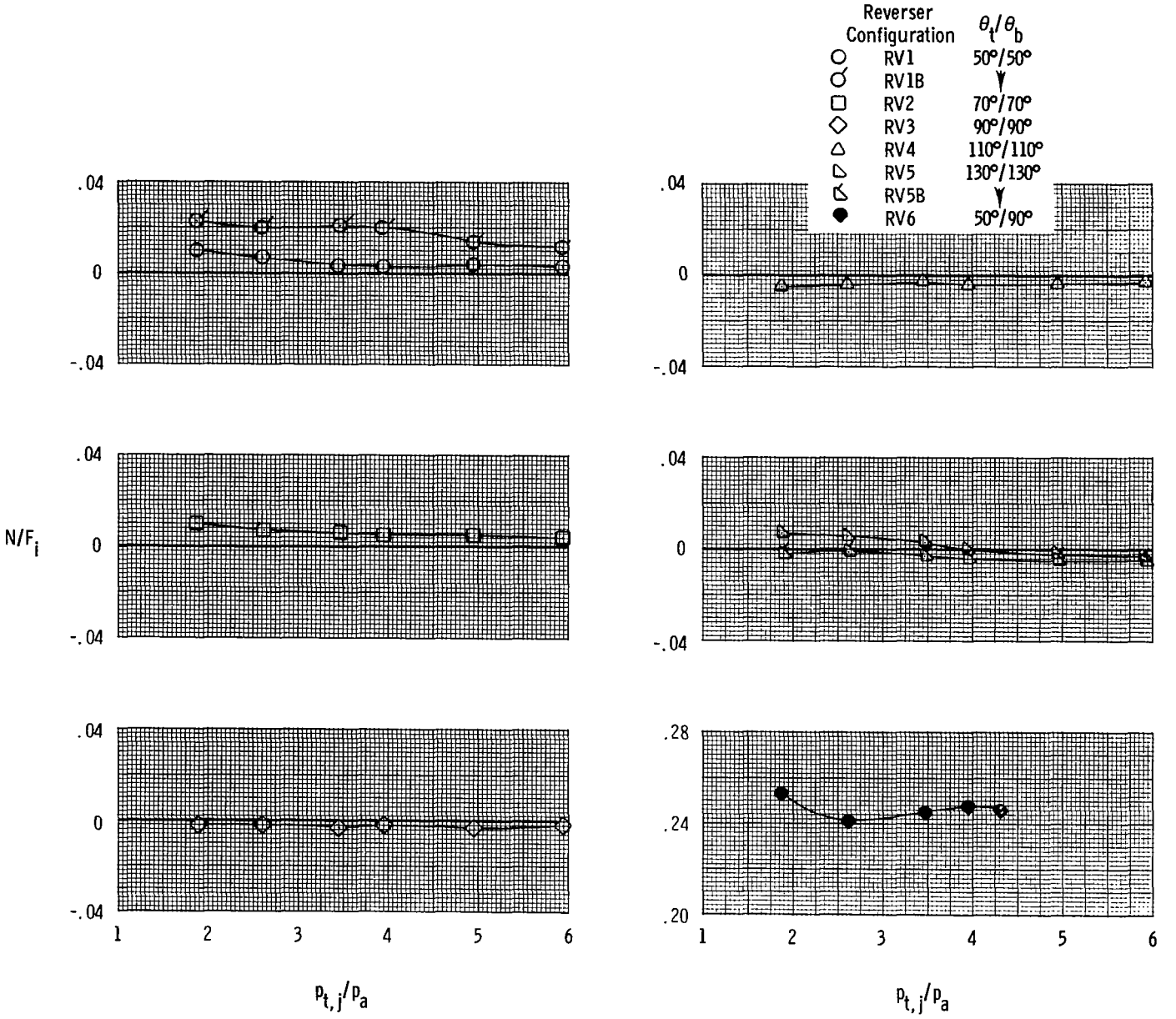

(b) Ratio of normal force to ideal thrust.

Figure 4.- Concluded.

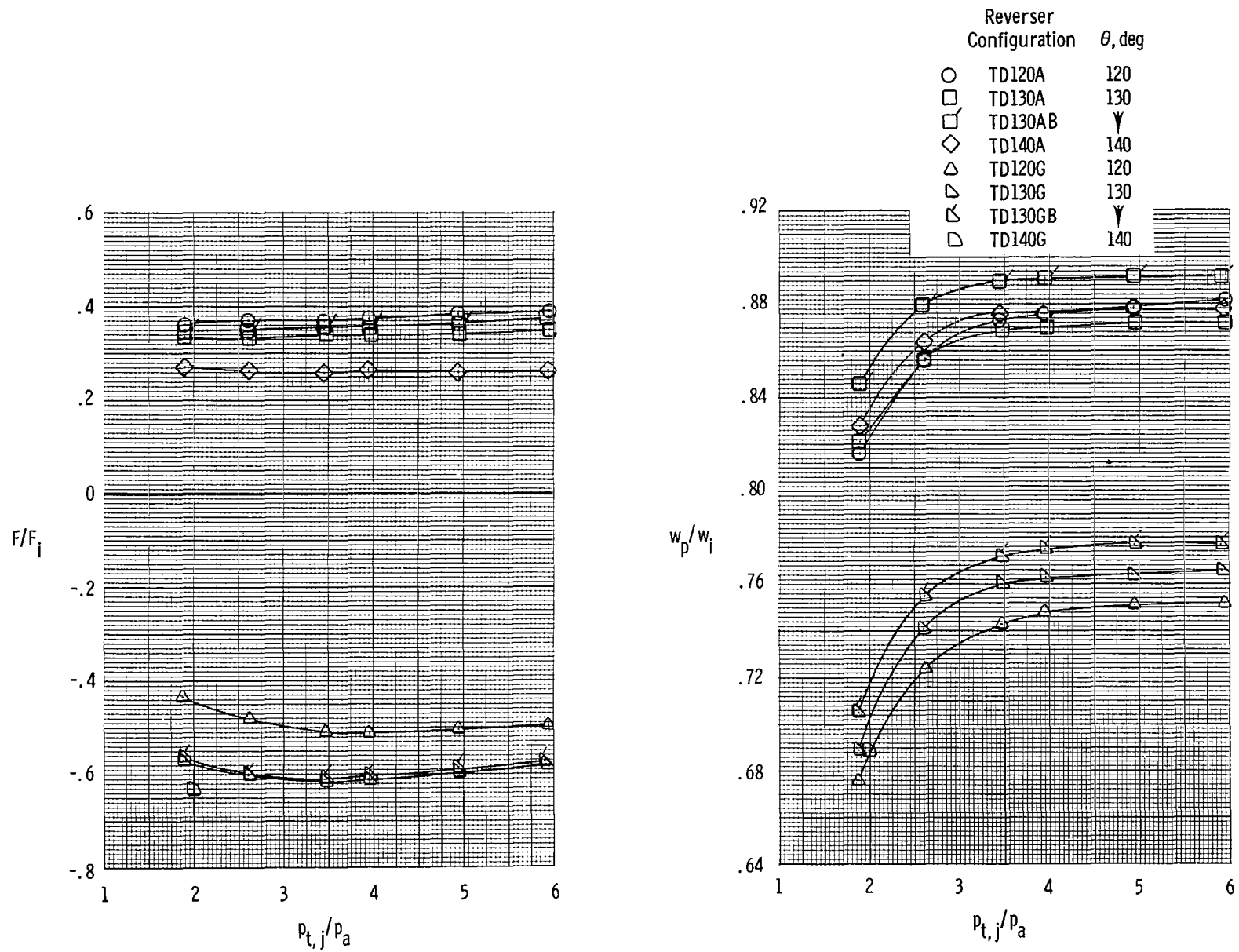

(a) Thrust ratio and discharge coefficient.

Figure 5.- Summary of static (M = 0) performance characteristics of three-door thrust-reverser concept. Tick marks represent area iterations ("B" configurations).

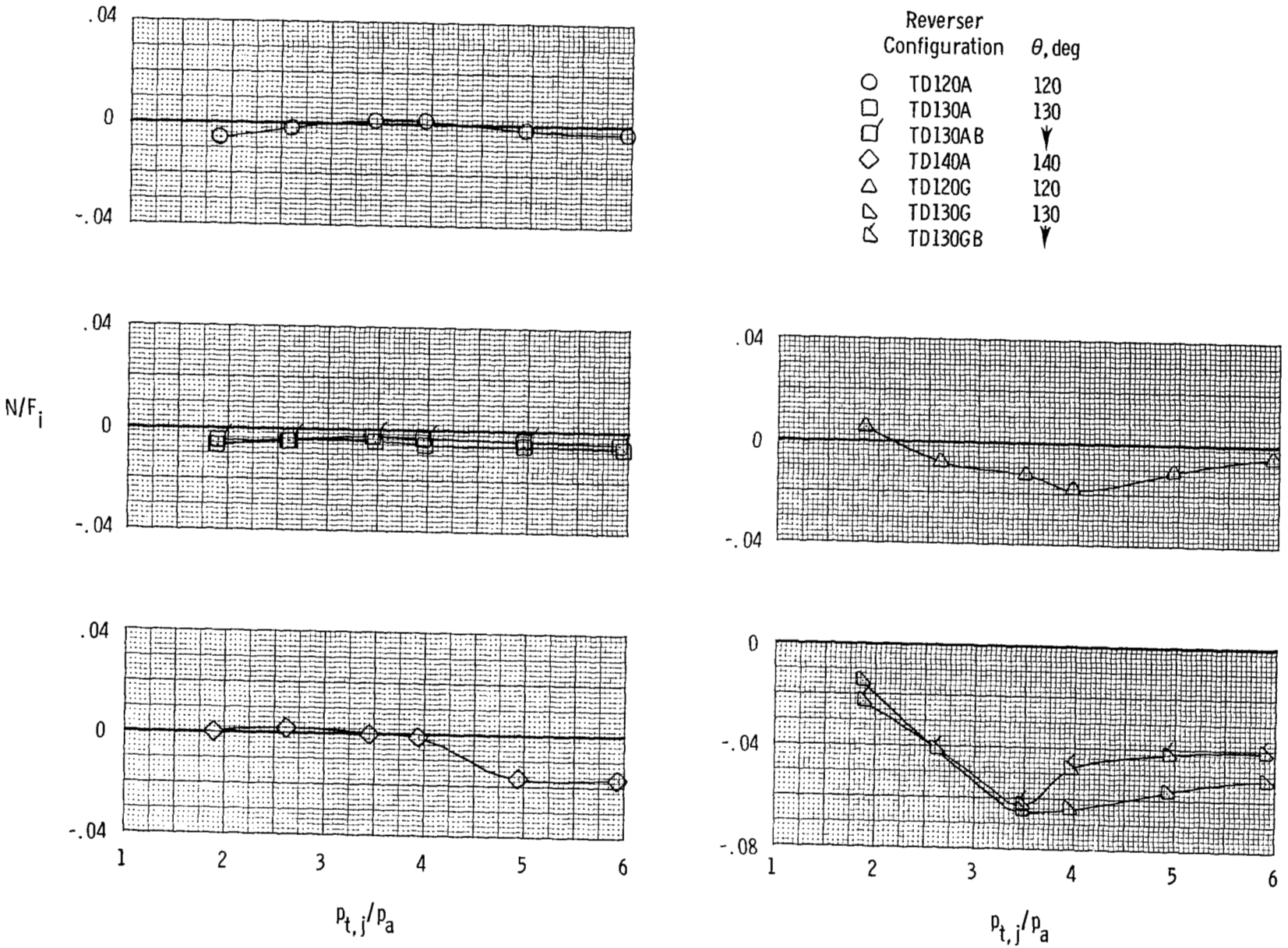

(b) Ratio of normal force to ideal thrust.

Figure 5.- Concluded.

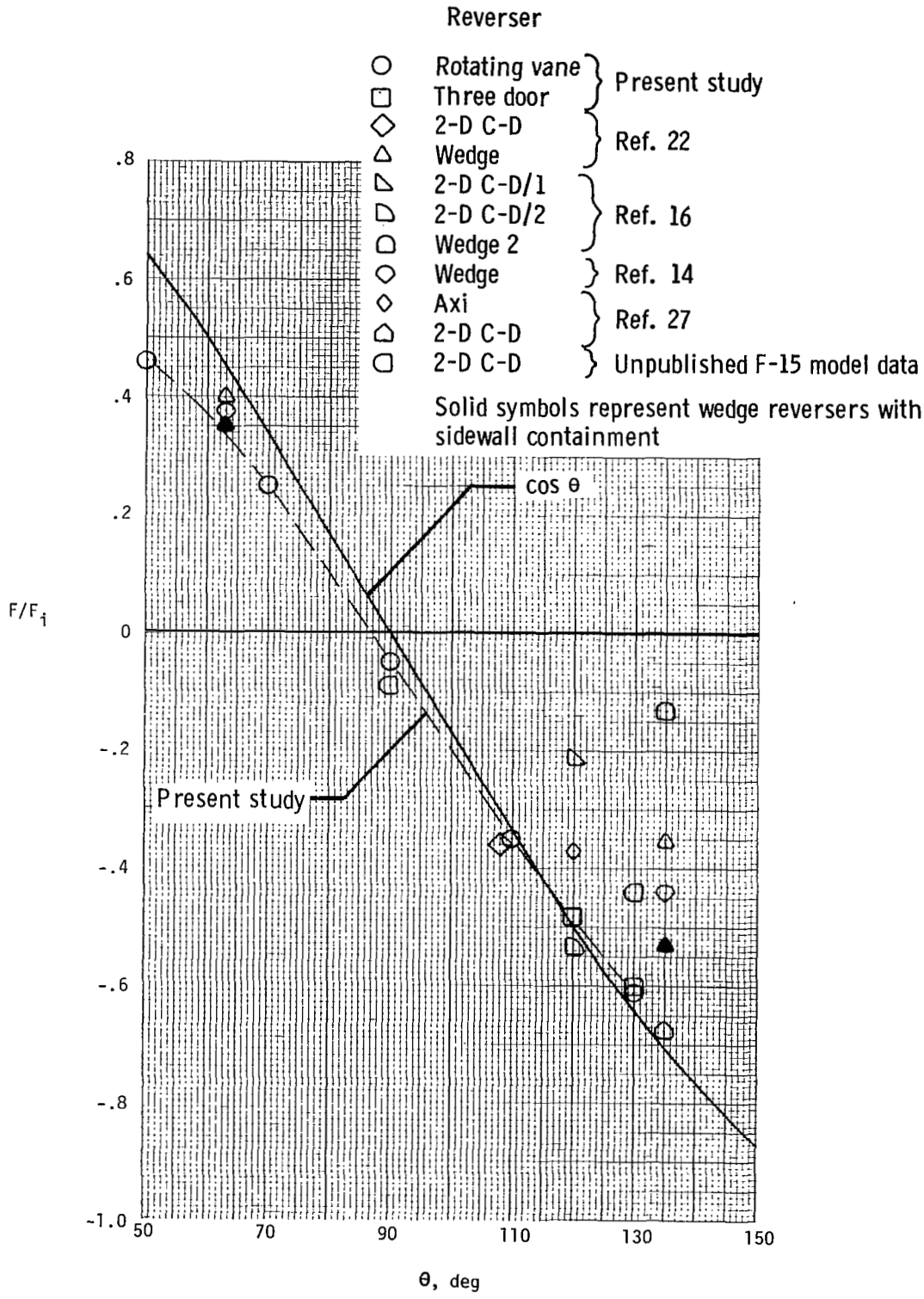

Figure 6.- Static performance versus geometric reverser angle for several axisymmetric and nonaxisymmetric reverser concepts. $p_{t,j}/p_a = 2.6$.

1. Report No.	2. Government Accession No.	3. Recipient's Catalog No.
NASA TP-2025		

4. Title and Subtitle	5. Report Date
STATIC INTERNAL PERFORMANCE CHARACTERISTICS OF TWO THRUST-REVERSER CONCEPTS FOR AXISYMMETRIC NOZZLES	June 1982
	6. Performing Organization Code: 505-43-23-01
7. Author(s): Laurence D. Leavitt and Richard J. Re	8. Performing Organization Report No.: L-15176
	10. Work Unit No.
9. Performing Organization Name and Address: NASA Langley Research Center, Hampton, VA 23665	11. Contract or Grant No.
	13. Type of Report and Period Covered: Technical Paper
12. Sponsoring Agency Name and Address: National Aeronautics and Space Administration, Washington, DC 20546	14. Sponsoring Agency Code

15. Supplementary Notes

16. Abstract

An investigation has been conducted in the static-test facility of the Langley 16-Foot Transonic Tunnel to determine the static performance of two axisymmetric-nozzle thrust-reverser concepts. A rotating-vane thrust reverser represented a concept in which reversing is accomplished upstream of the nozzle throat, and a three-door reverser concept provided reversing downstream of the nozzle throat. Nozzle pressure ratio was varied from 2.0 to approximately 6.0. The results of this investigation indicate that both the rotating-vane and three-door reverser concepts were effective static-thrust spoilers with the landing-approach nozzle geometry and were capable of providing at least a 50-percent reversal of static thrust when fully deployed with the ground-roll nozzle geometry.

17. Key Words (Suggested by Author(s))	18. Distribution Statement
Thrust reversing Thrust-reverser static performance Three-door thrust reverser Rotating-vane thrust reverser	Unclassified - Unlimited Subject Category 02

19. Security Classif. (of this report)	20. Security Classif. (of this page)	21. No. of Pages	22. Price
Unclassified	Unclassified	22	A02

For sale by the National Technical Information Service, Springfield, Virginia 22161

NASA-Langley, 1982